Polymer Chemistry

Accepted Manuscript

ROYAL SOCIETY OF CHEMISTRY

www.rsc.org/polymers

Cite this: DOI: 10.1039/c0xx00000x

www.rsc.org/xxxxxx

ARTICLE TYPE

Folic acid-functionalized AIE Pdots based on amphiphilic PCL-b-PCL for targeted cell imaging

Yan Zhang[a], Yujue Chen[b], Xing Li[a], Jibo Zhang[a], Jinlong Chen[a], Bin Xu[a]*, Xueqi Fu[b], Wenjing Tian[a]*

Received (in XXX, XXX) Xth XXXXXXXXX 20XX, Accepted Xth XXXXXXXXX 20XX

DOI: 10.1039/b000000x

Abstract

Fluorescent block amphiphilic copolymers are one of the most important bioimaging materials which are highly desirable for early stage cancer diagnosis and treatment. However, sometimes the application of the fluorescent block copolymers is severely limited because of the aggregation-caused quenching (ACQ) effect. Hereon, new aggregation induced emission polymer dots (AIE Pdots) were prepared through self-assembly process by using AIE-conjugated block copolymer containing AIE fluorophore, 9,10-bis(4-hydroxystyryl)anthracene, hydrophobic poly(ε-caprolactone) segments, hydrophilic poly(ethylene glycol) segments and folate groups. The AIE Pdots are monodispersed in H_2O with the average diameter of 15 nm, and possess strong emission and high solid state fluorescence quantum efficiency (Φ = 27.0%). Furthermore, the AIE Pdots show good stability and little toxicity to living cells and thus can be utilized for targeted HeLa cell imaging. Biological imaging investigation indicated that the folic acid functionalized AIE Pdots can be applied for targeted Hela intracellular imaging.

Introduction

Fluorescent polymer dots (FPdots), formed by amphiphilic block copolymers with hydrophobic cores and hydrophilic coronas, were used for observing biological processes, clinical imaging, metabolism and pharmacokinetics, as well as for the diagnosis/detection of disease and cancer formation either in vitro or in vivo.[1-6] However, the fluorescent intensity of the obtained FPdots will be significantly weakened in aqueous solution when the concentration become larger because of the aggregation-caused quenching (ACQ) effect, which limits the applications of FPdots for bioimaging.

Recently, aggregation-induced emission (AIE), a new category of fluorophores with exactly the opposite characteristic to ACQ, has been developed. Different from the notorious ACQ effect, AIE-active fluorophores are non-emissive in molecularly dissolved states while give highly fluorescent emission when they are in aggregate states.[7-9] Previous studies revealed that AIE luminogens are ideal candidates for the fabrication of FPdots with high fluorescence quantum efficiencies due to their efficient emission in aggregate state,[6, 10-27] and the encapsulation of AIE luminogens by amphiphilic block copolymer is a convenient way to fabricate AIE Pdots. Many encapsulating AIE Pdots showing good biological imaging capability have been prepared,[10-16] but unfortunately, there unavoidably present dye leakage, resulting in the cytotoxicity when applied in bioimaging. To overcome the leakage of dye, people prepared AIE Pdots by chemically coupling AIE fluorophores to the amphiphilic block copolymers (AIE amphiphilic block copolymers). For example, Y.Wei etal. synthesized two kinds of amphiphilic polymers through reversible addition fragmentation chain transfer polymerization with AIE fluorophore (R-E or PhE) and PEGMA as the monomers for cell imaging.[28, 29] B.Z.Tang etal. synthesized an quaternized amphiphilic polymer bearing tetraphenylethene (TPE) moiety and these polymers were able to internalize to the cells.[23] In addition, they used TPE to label chitosan (TPE-CS) chain and the aggregates of TPE-CS can be readily internalized by cells without leaking out for long-term fluorescent cellular tracing.[18, 23] Similarly, we also prepared two kinds of amphiphilic random copolymers with AIE luminogens (9,10-distyrylanthracene) based on free radical polymerization and applied them as fluorescent biological probes.[20, 21] However, almost all AIE amphiphilic block polymers reported did not have the ability to identify specific cells.

Herein, a new AIE Pdots for targeting Hela cells were developed. These monodispersed AIE Pdots can be easily prepared through self-assembly process by using AIE conjugated amphiphilic copolymers which contains AIE fluorophore, 9,10-bis(4-hydroxystyryl)anthracene (DSA), hydrophobic poly(ε-caprolactone) segments, hydrophilic poly(ethylene glycol) segments and folate groups. The poly(ε-caprolactone), a biodegradable material with good biocompatibility[30, 31] was served as the hydrophobic segment, and the biocompatible material poly(ethylene glycol) was served as the hydrophilic segment and folate groups acted as specifically targeted groups. The AIE Pdots have good chemical stability and colloidal stability, which indicates that no dye leakage phenomenon was found due to the stable chemical bond between DSA and PCL-b-PEG. This AIE Pdots possess strong emission and high solid state fluorescence quantum efficiency. The biocompatibility and cell

uptake behavior of the folic acids modified AIE Pdots were further investigated by two cell lines (HeLa cells and 3T3-L1 cells), which indicated that the folic acids modified AIE Pdots pose little toxicity to living cells and can be applied for targeted HeLa intracellular imaging.

Results and discussions

Design and synthesis of block copolymers P3 and P4

New AIE-conjugated PCL-b-PEG block copolymers (P3 and P4) bearing self-assembling properties were prepared as shown in Scheme 1. Compound 4 which has two hydroxyl groups was used as initiator for the polymerization of ε-caprolactone to prepare P1 through the typical ring-opening polymerization.[32, 33] P1 was activated by using p-nitrophenyloxycarbonyl chloride to afford polymer P2 which has two active nitrophenyl esters. P2 was then reacted with α,ω-diaminopolyethylene glycol (PEG, Mn = 2000) which has two amino end groups to get P3. In order to increase the ability of specific recognition to the block copolymer P3, folic acid was modified to the terminal (P4). ^{1}H NMR data were used for the degree of polymerization calculation while the relative molecular weights were measured by GPC using linear polystyrenes as standards.

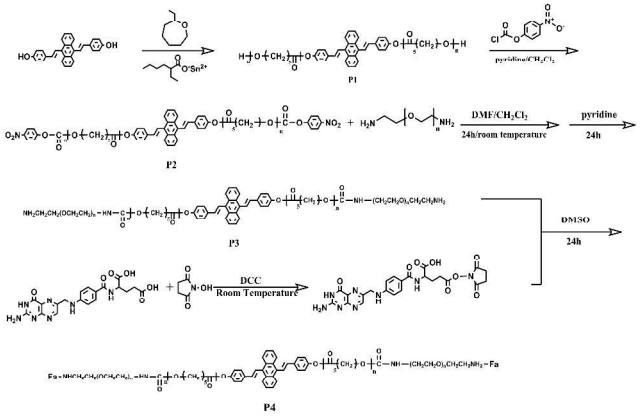

Scheme 1 Synthetic route.

Preparation and characterization of AIE Pdots

Taking advantage of the amphiphilic properties from copolymer P3 and P4, AIE Pdots could be easily prepared when H_2O was slowly dropped into the THF solution of the above two copolymers, as shown separately in Scheme 2. The PCL segments and AIE fluorophore 4 are encapsulated as the core while PEG segments distributed on the surface as the shell of the AIE Pdots in water. Therefore this method was feasible to enable the application of hydrophobic fluorophores in biocompatible environment by taking the advantages of the nanoparticles.

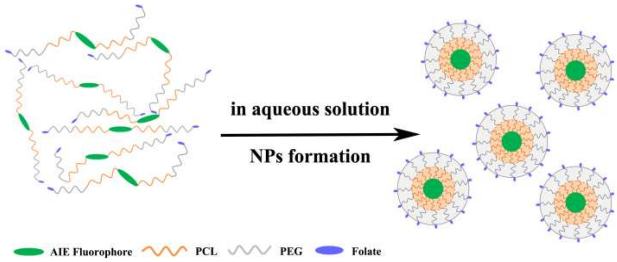

Scheme 2 Schematic drawing of the preparation of AIE Pdots.

P3 Pdots had regular sphere in morphology and uniform particle size, which means P3 Pdots have good monodispersity as shown in Fig.1 A. Similar results can be observed on P4 Pdots as shown in Fig.1 B and C. The diameter of P3 Pdots was about 9 nm and the particle size of P4 Pdots was around 16 nm. The reason for the larger diameter of P4 Pdots than that of P3 Pdots maybe origin from the modification of folic acids. The folic acids can increase the molecular weight of P4 compared with P3. In addition, folate groups on the surface of P4 Pdots could tend to form the hydrogen bonds between amine from folate group and water. These hydrogen bonds will make PEG segments stretch into water easily and result in increased the diameter of P4 Pdots.

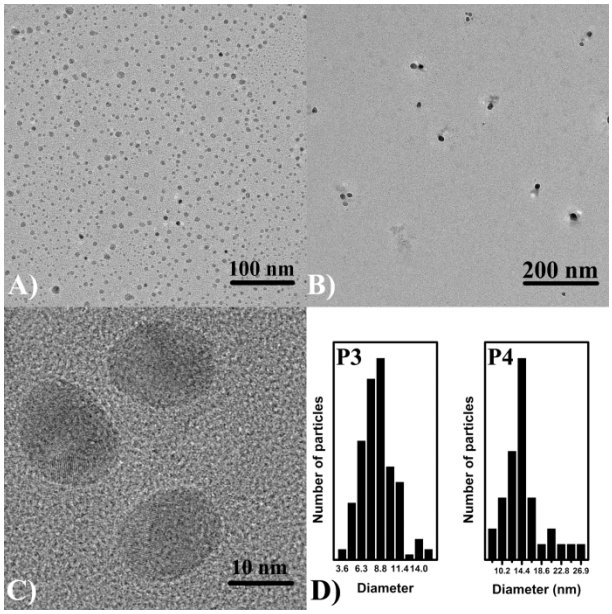

Fig. 1 A) TEM image of P3 Pdots with particle diameter around 9 nm and B) TEM image of P4 Pdots with particle diameter about 16 nm. C) Enlarge the image of P4 Pdots. D) Diameter statistics of two AIE Pdots.

Stability of AIE Pdots

The AIE-conjugated block copolymers possessed high chemical stability due to the covalent bond between AIE luminogens and PCL-b-PEG. After Placed in the dryer for 3 months, no change could be found from the ^{1}HNMR, which demonstrated the polymers were chemically stable. Meanwhile the AIE dots which were prepared by AIE-conjugated block copolymer were also very stable. To examine the stability of AIE Pdots, both P3 Pdots and P4 Pdots had been dialyzed against the regenerated cellulose membrane for 10 days without water change. Then the PL spectra of dialysates were measured as shown in Fig S3. Compared with

the PL spectra of Milli-Q water, the PL spectra of these two dialysates were almost the same as the Milli-Q water. And no fluorescence were found from the dialysates, which proved that AIE Pdots had good stability without any dye leakage.

The AIE Pdots also had excellent colloidal stability. The P4 Pdots suspension was very clear after it had been stored at room temperature for 30 days and at the same time, a few aggregations were found in P4 Pdots suspension. According to classic DLVO theory,[34, 35] colloidal stability was closely related to the surface potential. Therefore the surface charges of these two AIE Pdots were studied by zeta potential analysis. As shown in Fig.2, P3 Pdots exhibited positively signed ζ potentials at low pH (less than about 7.5), and the ζ potential curve was above zero due to the protonation of the amino groups. However, the ζ potential occurred inversion at high pH value (greater than about 7.5) because of the deprotonation of the amino groups.[36] In addition, P4 Pdots possessed negative charges due to the carboxyl on their surface from folate groups.[37] At neutral pH value (around 7), the ζ potentials of P4 and P3 Pdots were about -40 and 7 mV respectively, which further proved that P4 Pdots had higher colloidal stability than P3 Pdots.

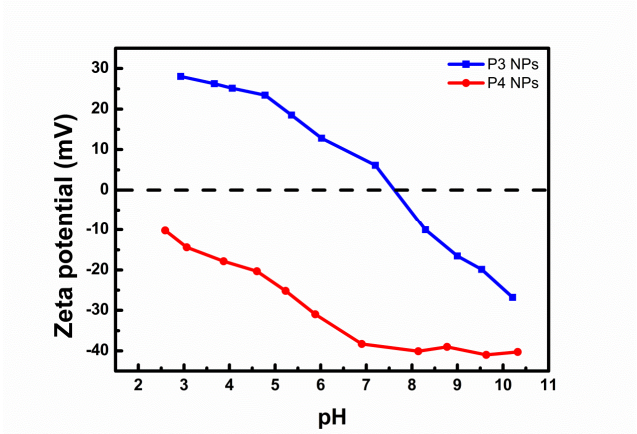

Fig. 2 Zeta potential of P3 Pdots (the blue line) and P4 Pdots (the red line) in the aqueous media with different pH at room temperature. Concentration: 0.5 mg/mL.

Photophysical properties

Fig.3 showed photophysical properties of the two copolymers and AIE Pdots. The AIE Pdots were prepared by slowly adding H_2O to their THF solutions, and the ratio of THF/ H_2O was 1:9. From the normalized absorbance spectra, the absorption peaks of the two copolymers solutions and the AIE Pdots solutions were all at about 410 nm. Compared to the absorption of P3, the enhancement of absorption of P4 at short wavelength region (less than 390 nm) could be attributed to the absorption superposition of the folate group and DSA.[38] A little band edge lift can be observed from the THF/H_2O mixed solution of P3 and P4, indicating that AIE Pdots had been formed according to Mie Scattering Theory.[39, 40]

The PL spectra of the two copolymers (P3 and P4) in THF and AIE Pdots dissolving in the THF/H_2O solvent are shown in Fig.3. It could be clearly observed that the fluorescence emissions of AIE Pdots are enhanced to their copolymers. As reported in our early research,[24, 26, 41-43] the significant twisted conformations of DSA derivatives can easily lead to the intramolecular vibration and rotation. DSA derivatives emit weak fluorescence in their good solution. Whereas, the aggregation of DSA derivatives emit strong fluorescence originated from the restriction of the intramolecular vibration and rotation.[15, 16] Thus, the enhancement emission behaviour of AIE Pdots was caused by the spatial confinement which restricts the intramolecular rotation of fluorophores (DSA) and the hydrophobic segments (PCL) of AIE Pdots. Fluorescence quantum yields (Φ) of the two copolymers in solutions were recorded by using quinine sulphate in 1.0 N H_2SO_4 as reference. And the AEE behaviour was clearly depicted by the relative changes of the fluorescence quantum yields (Φ) as shown in table S1. The Φ of P4 increased dramatically from 9.3% in THF solution to 17.0% in THF/water mixture with 90% volume fraction of water. And similar result was observed on copolymer P3, which shows weak emission in dilute THF solution (Φ = 3.7%), but enhanced emission (Φ = 15.8%) by the formation of nanoaggregates in the THF/water mixtures. Compared the fluorescence quantum yields of P4 to that of P3, P4 yields higher fluorescence quantum both in THF solution and in the aggregation state. The different fluorescence quantum between P3 and P4 in THF may depend on the different molecular conformation. Compared with the stretch configuration of P3 in THF, the molecular chains of P4 tend to form a coil conformation due to the poor solubility of folic acid in THF. The closer configuration of P4 may restrict intramolecular vibration and rotation in some degree and therefore, enhanced the emission of P4. In the meantime, the nano-aggregates of P4 get higher fluorescence quantum yields, which put down to the higher level of aggregation induced by the folic acids.[8, 9] Because of the poor solubility of folic acid in water (neutral pH environment), the introduction of the folic acid will provide a hydrophobic environment, and thus the aggregation of the copolymer P4 is enhanced. Therefore, the aggregations of AIE fluorophores could be manipulated and high quantum yields could be achieved. Furthermore, the solid state fluorescence quantum yields of the powders of P3 Pdots and P4 Pdots measured with integrating sphere were 18.0% and 27.0%, respectively, which make the AIE Pdots possess potential in the biological applications.

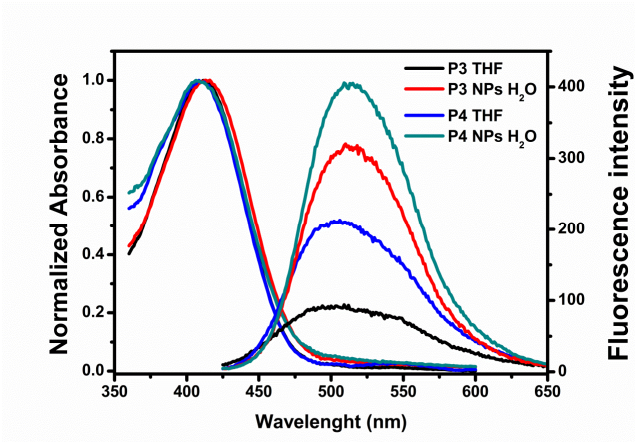

Fig. 3 Normalized UV–vis absorption and PL spectra of P3, P4 THF solution and THF/H_2O mixed solution. The ratio of THF/H_2O is 1:9 and all the concentrations are 0.2 μM.

Cytotoxicity

Methylthiazolyldiphenyltetrazolium (MTT) assay was adapted to investigate the cytotoxicity of P3 and P4 by studying the metabolic viability of Hela cells after incubation with P3 Pdots and P4 Pdots at various concentrations as shown in Fig.4. For these two AIE Pdots, slight concentration and time dependence cytotoxicity were observed. The cell viability of P3 Pdots remains 76% by using a polymer concentration of 400 μg/mL after cellular internalization of 48 h and the cell viability of P4 Pdots was about 83%, which indicates low cytotoxicity of the AIE Pdots.

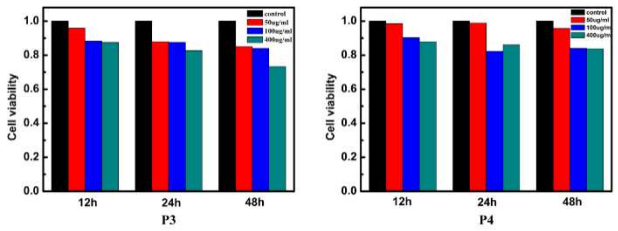

Fig. 4 Cytotoxicity of P3 Pdots and P4 Pdots to Hela cells incubated for different time.

Bioimaging

These AIE Pdots are expected as good candidates for biological imaging due to their suitable size, good stability and good luminescence performance. To evaluate the performance of specific cellular imaging of these AIE Pdots, Hela cells (human cervical epithelioid carcinoma) with over-expressing folate receptor (FR) were chosen for the imaging experiments as target cells. Meanwhile, 3T3-L1 cells (mice preadipocytes cells) with low expression of folate receptors were chosen for control experiments.

Application of the prepared P3 and P4 Pdots in cellular imaging was investigated by confocal laser scanning microscopy (CLSM). Hela cancer cells and 3T3-L1 cells had been incubated in culture medium with two AIE Pdots suspensions for 3 h, 7 h, and 16 h at the concentration of 0.16 mg/mL. The CLSM images of Hela cancer cells after incubation with P3 Pdots are shown in Fig.5 G-L. There were almost no fluorescence found when P3 Pdots had been incubated for 3 h and only weak fluorescence could be found in cytoplasm when P3 Pdots had been incubated for 7 h (Fig.5 I-L). Strong fluorescence could be found in cytoplasm with the continuous increasing of incubation time. In contrast, P4 Pdots are effectively internalized into cytoplasm of Hela cells by endocytosis (Fig.5 A-F), even if having been incubated for 3 h (Fig.5 E, F).

As reported that folic acid has been proved to be a useful molecule for targeting cancer cells, primarily because: (1) folate receptor (FR) is obviously over-expressed on many cancer cells, such as Hela cells and folate has high binding affinity to FR ($K_d \sim 10^{-10}$ M), (2) access to FR in those normal tissues express that it can be severely limited due to the location of FR on the apical (externally-facing) membrane of polarized epithelia, (3) FR density appears to increase in the cancer worsens.[29, 32] Thus, folates are distributed in the surface of P4 Pdots and fast bonding to FR in Hela cells, leading to a faster incubation rate than that of P3 Pdots.

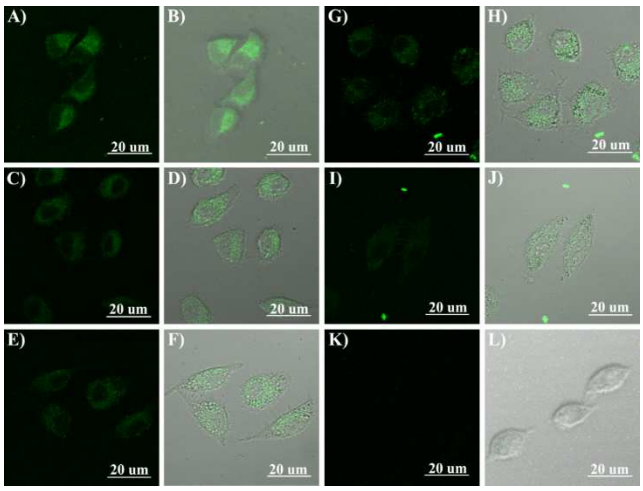

Fig. 5 Confocal fluorescence images of AIE Pdots for Hela cells; A)-F) were P4 Pdots for HeLa Cells; G)-L) were P3 Pdots for Hela cells. A), B), G), H) were incubated for 16 h; C), D), I), G) were incubated for 7 h; E), F), K), L) were incubated for 3 h. Incubated concentrations of AIE Pdots were 0.16 mg/mL. Excitation light: 405 nm.

To further prove the fact that P4 Pdots have the ability of specific recognition to Hela cells, we conducted the experiment with 3T3-L1 cells which have only few FR by incubating P4 Pdots for 3 h, 7 h, 16h under controlling experiments condition. After incubating 3h, almost no fluorescence signal was found (Fig.6 A and D). The low internalization rate of P4 Pdots was ascribed to the low expression of folate receptors in 3T3-L1 cell membrane. With the extension of the incubation time, the cells were gradually lighted up through the endocytosis process observed by confocal fluorescence images (Fig.6 B, C, E, F).[37] Although there were only a few FR on the cell surface, with the increase of incubation time, some of P4 Pdots by endocytosis gradually access into 3T3-L1 cells. These results sufficiently support the specific targeting ability of P4 Pdots to folate receptor-overexpressed cancer cells because of the folic acid-functionalized surface.

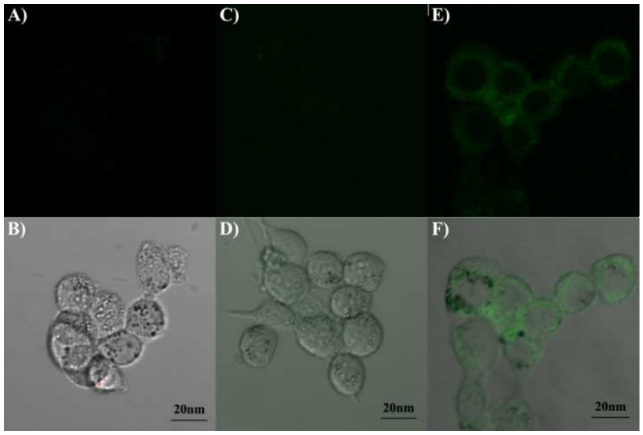

Fig. 6 Confocal fluorescence images of P4 Pdots for 3T3-L1 cells. A), D) were incubated for 16 h; B), E) were incubated for 7 h; C), F) were incubated for 3 h. Incubated concentration of P4 Pdots were 0.16 mg/mL. Excitation light: 405 nm.

Conclusion

New AIE Pdots which have the ability to targeted Hela cells with high fluorescence quantum efficiency were prepared. These monodispersive AIE Pdots can be easily prepared through self-assembly process by using AIE conjugated amphiphilic copolymer which contains an AIE fluorophore, 9,10-bis(4-hydroxystyryl) anthracene (DSA), hydrophobic poly(ε-caprolactone) segments, hydrophilic poly(ethylene glycol) segments and folate groups. The self-assembled AIE Pdots are stable in aqueous solution with the average diameters of 15 nm. The AIE Pdots have high fluorescence quantum efficiency (Φ = 27.0%). Moreover, the folic acid functionalized AIE Pdots show targeting ability to Hela cells which overexpress the folate receptor. Therefore, the folic acids functionalized AIE Pdots can be applied for the targeted Hela intracellular imaging and provide a strategy to construct bright and highly photobleaching resistant fluorescent probes.

Experimental

Materials and Reagents

α,ω-diaminopolyethylene glycol (Mn = 2000) was purchased from Aladdin Industrial Inc., and other general chemicals employed in this study were of the best grade available and were obtained from J&K Scientific Ltd, energy chemical Co. and used without further purification,unless otherwise noted. N,N'-dimethylformamide (DMF), tetrahydrofuran (THF) and methylene chloride ($CHCl_2$) were purified by fractional distillation before used as solvents. Deionized water (18.2 MΩ•cm resistivity) from a Milli-Q water system was used throughout the experiments.

Instruments

500 MHz ^{1}H NMR and 125 MHz ^{13}C NMR were recorded on a liquid NMR (BRUKER, AVANCEIII500) used for ^{1}H NMR spectra measurements. Mass spectra were recorded on an Agilent 1100 LC-MS system. IR spectra were recorded on Perkin-Elmer spectrophotometer in the 4000–400 cm^{-1} region through using a powdered sample on a KBr plate. Molecular weights of polymers were determined using a Pl-GPC-120 system from Polymer Laboratories Ltd, in reference with a series of polystyrene standards. Self-assembly process was completed with a micro-syringe pump (Lungerpump, LSP01-1A). Photo luminescence spectra were collected on a Shimadzu RF-5301PC spectrophotometer. UV-vis absorption spectra were recorded using a Shimadzu UV-3600 UV-vis spectrophotometer. Solid state PL efficiencies were measured by an integrating sphere (C-701, Labsphere Inc.) with a 405 nm Ocean Optics LLS-LED as the excitation source, and the laser was introduced into the sphere through the optical fiber. Transmission electron microscopy (TEM) images were obtained with a transmission electron microscope (TEM, JEM-2100F). Zeta potentials measurement was performed using a Brookhaven BI-90Plus particle size analyser at room temperature.

Synthesis

Synthetic route shown in scheme 1 was briefly described as follows and parts of structural characterization data were shown in supporting information.

Synthesis of 9,10-bis(4-hydroxystyryl)anthracene (4)

Specific synthesis and pure methods are listed in supporting information according to previously literature.[21] ^{1}H NMR (DMSO-d6, 25^{o}C, 400 MHz, TMS, ppm): δ = 9.67 (s, 2H), 8.32-8.34 (m, 4H), 7.83 (d, 2H), 7.60 (d, 4H), 7.48-7.51 (m, 4H), 6.82 (d, 4H), 6.77 (d, 2H); MS: $C_{30}H_{23}O_2$ (MtH), calcd. 415.1698; found 415.1699.

Synthesis of P1

Compound 4 (62.3 mg, 0.15 mmol) was weighed into a flask containing 1.5mL toluene and ε-caprolactone (1.03 g, 8.76 mmol) was subsequently added. Toluene was added to spread the solution. The reaction mixture had been stirred for 5 min at 110 ^{o}C in a preheated oil bath and then catalyst (stannous octoate, 1 drop) was added and the polymerization had been performed for 12 h. The resulting viscous solution was cooled, upon which it solidified. The crude polymer was dissolved in dichloromethane and precipitated into cold methanol. The isolated yield was 66%. Mn (NMR) = 8167. Degree of polymerization (DP) of PCL = 34.^{1}H NMR ($CDCl_3$, 25^{o}C, 500 MHz, TMS, ppm) δ = 8.34-8.38 (m, 4H), 7.92 (d, 2H), 7.83 (d, 2H), 7.72 (d, 2H), 7.61 (d, 2H), 7.46-7.51 (m, 4H), 7.11-7.21 (m, 2H), 6.88-6.97 (m, 4H), 4.07 (t, 136H), 2.34 (t, 136H), 1.8-1.3 (m, 408H).

Synthesis of P3

P1(310 mg, 0.038 mmol of the corresponding hydroxyl group), 50 mg of compound 8 (0.25 mmol), and 30 mg of pyridine (0.3 mmol) were dissolved in 10 mL of anhydrous methylene chloride and stirred at room temperature overnight to generate the intermediate P2 (289 mg) which was precipitated from the reaction mixture into ether filtered and dried. 450 mg of α,ω-Diaminopolyethylene glycol (Mn = 2000) (2.6 mmol of the free amino group) in 5 mL of dimethylformamide (DMF) was added into 10 mL P2 (289mg) containing methylene chloride and the mixture had been stirred at room temperature for 1 day. 1 mL of additional pyridine was added into the mixture and the reaction had been stirred for one more day.[45] The low boiling point solvent was removed under reduced pressure and then precipitation was used ether. Further purification was carried out using dialysis. The powder (289 mg) was dissolved in 250 mL of THF and the solution was slowly added to 150 mL of water to form the micelles. The mixture had been dialyzed against the regenerated cellulose membrane with a Mw cut off of 8000–12 000 for 1 week and then most of the water was removed under reduced pressure and dried in vacuo to get 150 mg of P3. The yield in dialysis process was calculated to be 52%. ^{1}H NMR ($CDCl_3$, 25^{o}C, 500 MHz, TMS, ppm) δ= 8.34-8.38 (m, 4H), 7.92 (d, 2H), 7.83 (d, 2H), 7.72 (d, 2H),7.61 (d, 2H), 7.46-7.51 (m, 4H), 7.11-7.21 (m, 2H), 6.88-6.97 (m, 4H),4.07 (t, 150H), 3.66 (m, 370H), 2.34 (t, 150H), 1.8-1.3 (m, 440H). Mn (GPC) = 11689, Mw/Mn = 1.59. Mn (NMR) = 12359. FTIR (ν, cm^{-1}): 2956, 2867 and 2928 (strong, CH_2, CH_3), 1721 (strong, -COO- of ester).

Synthesis of P4

Folic acid (4) (0.65 g, 1.47 mmol) was dissolved in 25 mL dimethylsulfoxide (DMSO). NHS (0.34 g, 2.9 mmol) and dicyclohexylcarbodiimide (DCC) (0.6 g, 2.9 mmol) were then added. The reaction was allowed to proceed over night at room temperature under stirring and shielded from light. Insoluble by-product was removed by filtration, and then precipitated in

diethyl ether to get N-hydroxysuccinimide (NHS) ester of folic acid. Then 20 mg P3 and 80 mg NHS-FA were dissolved in 10 mL DMSO and had reacted for 24 hours at room temperature. After that the reaction solution was added to 35 mL NaOH solution (pH = 9), and then P4 was obtained by centrifugation 12000 rpm for 10min. FTIR (ν, cm^{-1}): 2940 and 2883 (strong, CH_2, CH_3), 1721 (strong, -COO- of ester), 3327 (strong, -CON- of acidamide), 1645 and 1610 (strong and week, $-NH_2$ of acidamide).

Preparation of AIE Pdots

P3 (5 mg) was dissolved in THF (350 mL) and stirred for 30 min. 1.5 mL deionized water were injected by micro-syringe pump with injection rate at 12 μL/min into THF of P3 under stirring rate at 500 r/min to form AIE Pdots. The AIE Pdots had been dialyzed against deionized water for 5 days with a water change approximately every 12 h. The solution was then filtered through a 220 nm micro-filter to remove possible large particles before cell experiments. P4 Pdots were prepared with the similar method.

Determination of quantum yields

Fluorescence quantum yields (Φ) of samples in solutions were recorded by using quinine sulphate in 0.1M H_2SO_4 (Φ = 0.54excitation wavelength of 365 nm) and were calculated according to the following equation.[44]

$$\phi_s = \phi_r \left(\frac{A_r}{A_s}\right)\left(\frac{I_s}{I_r}\right)\left(\frac{n_r^2}{n_s^2}\right)$$

Where Φ_r and Φ_s are the fluorescence quantum yields of standards and the samples, respectively. A_r and A_S are the absorbance of the standards and the measured samples at the excitation wavelength, respectively. I_r and I_s are the integrated emission intensities of standards and the samples, respectively. n_r and n_s are the refractive indices of the corresponding solvents of the solutions.

Solid state PL efficiencies were measured with an integrating sphere[45] with a 405 nm Ocean Optics LLS-LED as the excitation source, and the laser was introduced into the sphere through the optical fiber.

Cell culture and imaging

HeLa cells and 3T3-L1 cells were cultured in minimum essential medium containing 10% fetal bovine serum and antibiotics (100 units per mL penicillin and 100 μg/mL streptomycin) in a 5% carbon dioxide humidity incubator at 37°C.

Cytotoxicity study

The cell proliferation Kit I (MTT) was used to measure the cell viability. First, 500 cells were seeded per well in a 96-well plate. After overnight culture, various concentrations of P3 Pdots and P4 Pdots were added into the 96-well plate. After 12h, 24 h, 48h. 10 μL of MTT solution (5 mg/mL in PBS) was added into each well. After 4 h incubation at 37°C, 50 μL of solubilization mixture containing 10% SDS and 0.01M HCl were added to dissolve the purple crystals. After 12 h, the absorbance was measured at 590 nm. Every experiment was performed at least three times.

Acknowledgements

This work is supported by 973 Program (2013CB834702), the Natural Science Foundation of China(No. 51373063, 21204027, 21221063), the Research Fund for the Doctoral Program of Higher Education of China (20120061120016) and the Project of Jilin Province (20100704).

Notes and references

[a] *State Key Laboratory of Supramolecular Structure and Materials, College of Chemistry, Jilin University, Changchun 130012, PR China. Email:*wjtian@jlu.edu.cn, xubin@jlu.edu.cn*; fax: +86-431-85193421*
[b] *Edmond H. Fischer Signal Transduction Laboratory, College of Life Sciences, Jilin University, Changchun 130012, P. R. China*

† Electronic Supplementary Information (ESI) available. See DOI:10.1039/b000000x/

1. S. W. Thomas, G. D. Joly and T. M. Swager, *Chem. Rev.*, 2007, **107**, 1339-1386.
2. R. Weissleder and M. J. Pittet, *Nature*, 2008, **452**, 580-589.
3. H. Kobayashi, M. Ogawa, R. Alford, P. L. Choyke and Y. Urano, *Chem. Rev.*, 2009, **110**, 2620-2640.
4. C. A. Traina, R. C. Bakus Ii and G. C. Bazan, *J. Am. Chem. Soc.*, 2011, **133**, 12600-12607.
5. N. Boens, V. Leen and W. Dehaen, *Chem. Soc. Rev.*, 2012, **41**, 1130-1172.
6. L. Feng, C. Zhu, H. Yuan, L. Liu, F. Lv and S. Wang,*Chem. Soc. Rev.*, 2013, **42**, 6620-6633.
7. J. Luo, Z. Xie, J. W. Y. Lam, L. Cheng, H. Chen, C. Qiu, H. S. Kwok, X. Zhan, Y. Liu, D. Zhu and B. Z. Tang, *Chem. Commun.*, 2001, 1740-1741.
8. Y. Hong, J. W. Y. Lam and B. Z. Tang,*Chem. Soc. Rev.*, 2011, **40**, 5361-5388.
9. A. Qin, J. W. Y. Lam and B. Z. Tang, *Prog. Polym. Sci.*, 2012, **37**, 182-209.
10. J. Geng, K. Li, W. Qin, L. Ma, G. G. Gurzadyan, B. Z. Tang and B. Liu, *Small*, 2013, **9**, 2012-2019.
11. D. Wang, J. Qian, S. He, J. S. Park, K.S. Lee, S. Han and Y. Mu, *Biomaterials*, 2011, **32**, 5880-5888.
12. W.C. Wu, C.Y. Chen, Y. Tian, S.H. Jang, Y. Hong, Y. Liu, R. Hu, B. Z. Tang, Y. T. Lee, C.T. Chen, W.C. Chen and A. K. Y. Jen, *Adv. Funct. Mater.*, 2010, **20**, 1413-1423.
13. Y. Yang, F. An, Z. Liu, X. Zhang, M. Zhou, W. Li, X. Hao, C. S. Lee and X. Zhang, *Biomaterials*, 2012, **33**, 7803-7809.
14. X. Zhang, X. Zhang, S. Wang, M. Liu, L. Tao and Y. Wei, *Nanoscale*, 2013, **5**, 147-150.
15. Q. Zhao, K. Li, S. Chen, A. Qin, D. Ding, S. Zhang, Y. Liu, B. Liu, J. Z. Sun and B. Z. Tang, *J. Mater. Chem.*, 2012, **22**, 15128-15135.
16. Z. Zhao, J. Geng, Z. Chang, S. Chen, C. Deng, T. Jiang, W. Qin, J. W. Y. Lam, H. S. Kwok, H. Qiu, B. Liu and B. Z. Tang, *J. Mater.Chem.*, 2012, **22**, 11018-11021.
17. F. Anariba, L. L. Chng, N. S. Abdullah and F. E. H. Tay, *J. Mater. Chem.*, 2012, **22**, 19303-19310.
18. M. Li, Y. Hong, Z. Wang, S. Chen, M. Gao, R. T. K. Kwok, W. Qin, J. W. Y. Lam, Q. Zheng and B. Z. Tang, *Macromol. Rapid Comm.*, 2013, **34**, 767-771.
19. S. J. Lim, B. K. An, S. D. Jung, M. A. Chung and S. Y. Park, *Angew. Chem. Int. Ed.*, 2004, **43**, 6346-6350.
20. H. Lu, F. Su, Q. Mei, Y. Tian, W. Tian, R. H. Johnson and D. R. Meldrum, *J. Mater. Chem.*, 2012, **22**, 9890-9900.
21. H. Lu, F. Su, Q. Mei, X. Zhou, Y. Tian, W. Tian, R. H. Johnson and D. R. Meldrum, *J. Polym. Sci. Pol. Chem.*, 2012, **50**, 890-899.
22. A. Qin, Y. Zhang, N. Han, J. Mei, J. Sun, W. Fan and B. Z. Tang, *Sci. China Chem.*, 2012, **55**, 772-778.
23. Z. Wang, S. Chen, J. W. Y. Lam, W. Qin, R. T. K. Kwok, N. Xie, Q. Hu and B. Z. Tang, *J. Am. Chem. Soc.*, 2013, **135**, 8238-8245.
24. J. Chen, S. Ma, B. Xu, J. Zhang, Y. Dong and W. Tian, *Chin. Sci. Bull.*, 2013, **58**, 2747-2752.

25. Z. Wang, K. Ma, B. Xu, X. Li and W. Tian, *Sci. China Chem.*, 2013, **56**, 1234-1238.
26. J. Zhang, B. Xu, S. Ma, J. Chen, Y. Dong, W. Tian, *Prog. Chem.*, 2013, **25**, 1079-1089.
27. X. Li, B. Xu, H. Lu, Z. Wang, J. Zhang, Y. Zhang, Y. Dong, K. Ma, S. Wen and W. Tian, *Anal. Methods*, 2013, **5**, 438-441.
28. X. Zhang, X. Zhang, B. Yang, M. Liu, W. Liu, Y. Chen and Y. Wei, *Polym. Chem.*, 2014, **5**, 356-360
29. X. Zhang, M. Liu, B. Yang, X. Zhang, Z. Chi, S. Liu, J. Xu and Y. Wei, *Polym.Chem.*, 2013, **4**, 5060-5064.
30. D. B. Shenoy, R. J. D'Souza, S. B. Tiwari and N. Udupa, *Drug Dev. Ind.Pharm.*, 2003, **29**, 555-563.
31. D. Rohner, D. Hutmacher, P. See, K. Tan, V. Yeow, S. Tan, S. Lee and B. Hammer, Mund. Kiefer.Gesichtschir., 2002, **6**, 162-167.
32. X. He, L. Liang, M. Xie, Y. Zhang, S. Lin and D. Yan, *Macromol.Chem. Phys.*, 2007, **208**, 1797-1802.
33. M. A. R. Meier, S. N. H. Aerts, B. B. P. Staal, M. Rasa and U. S. Schubert, *Macromol.Rapid. Comm.*, 2005, **26**, 1918-1924.
34. E. J. W. Verwey, *J. Phys. Colloid. Chem.*, 1947, **51**, 631-636.
35. B. Derjaguin and L. Landau, *Prog. Surf. Sci.*, 1993, **43**, 30-59.
36. A. K. Peacock, S. I. Cauet, A. Taylor, P. Murray, S. R. Williams, J. V. M. Weaver, D. J. Adams and M. J. Rosseinsky, *Chem. Commun.*, 2012, **48**, 9373-9375.
37. Z. Wang, B. Xu, L. Zhang, J. Zhang, T. Ma, J. Zhang, X. Fu and W. Tian, *Nanoscale*, 2013, **5**, 2065-2072.
38. M. Poe, *J. Biol. Chem.*, 1977, **252**, 3724-3728.
39. P. Galletto, P. F. Brevet, H. H. Girault, R. Antoine and M. Broyer, *J. Phys. Chem. B*, 1999, **103**, 8706-8710.
40. G. Mie, *Ann. Phys.(Berlin)*, 1908, **330**, 377-445.
41. Y. Dong, B. Xu, J. Zhang, X. Tan, L. Wang, J. Chen, H. Lv, S. Wen, B. Li, L. Ye, B. Zou and W. Tian, *Angew. Chem. Int. Ed.*, 2012, **51**, 10782-10785.
42. L. Wang, B. Xu, J. Zhang, Y. Dong, S. Wen, H. Zhang and W. Tian, *Phys. Chem. Chem. Phys.*, 2013, **15**, 2449-2458.
43. J. Zhang, J. Chen, B. Xu, L. Wang, S. Ma, Y. Dong, B. Li, L. Ye and W. Tian, *Chem. Commun.*, 2013, **49**, 3878-3880.
44. Y. Tian, W.C. Wu, C.Y. Chen, T. Strovas, Y. Li, Y. Jin, F. Su, D. R. Meldrum and A. K. Y. Jen, *J. Mater. Chem.*, 2010, **20**, 1728-1736.
45. J. C. de Mello, H. F. Wittmann and R. H. Friend, *Adv. Mater.*, 1997, **9**, 230-232.

Folic acid-functionalized polymer dots with aggregation induced emission feature (AIE Pdots) with show high fluorescence efficiency and little toxicity to living cells, which possess a good capability for targeted Hela intracellular imaging.